ISSN: 2277-9655
Impact Factor: 4.116

IJESRT

INTERNATIONAL JOURNAL OF ENGINEERING SCIENCES & RESEARCH TECHNOLOGY

VALIDATION OF SINGLE POINT INCREMENTAL FORMING PROCESS FOR DEEP DRAWN PYRAMIDAL CUPS USING EXPERIMENTAL GRID-BASED DEFORMATION

Chennakesava R Alavala
Department of Mechanical Engineering, JNT University Hyderabad, India

DOI: 10.5281/zenodo.60091

ABSTRACT

The use of finite element analysis in manufacturing has enabled the development of several new sheet metal forming processes. Recent advances have enabled the localized deformation to be accurately controlled using CNC technology. Single point incremental forming has the potential to revolutionize sheet metal forming, making it accessible to all levels of manufacturing. This paper describes the validation of single point increment forming of pyramidal cups with the experimental grid-based deformation. The present investigation confirms that the FLD is sensitive to strain path of aluminum alloy 2004.

KEYWORDS: Single point incremental forming, finite element analysis, AA2004, pyramidal cups, grid-based deformation, formability limit diagram.

INTRODUCTION

In metal forming processes, the product shapes are produced by plastic deformation. Sheet metal is used by a number of manufacturers for producing a large variety of household and industrial products. The most commonly used sheet forming process is cold drawing, which converts flat blanks into parts whose shape is composed of surfaces that cannot be obtained by simple bending. The formed part is often referred to as a shell or cup, and must conserve a good surface condition, without local thinning or wrinkling [1]. By convention, any type of deformation in a sheet [2-5] can be represented by a point in the ε_1 vs ε_2 diagram shown in figure 1, where ε_1 is the principal strain in the plane of the sheet and ε_2 is the strain perpendicular to ε_1. The thickness strain ε_3 is obtained from the law of conservation of volume:

$$\varepsilon_1 + \varepsilon_2 + \varepsilon_3 = 0 \quad (1)$$

ISSN: 2277-9655
Impact Factor: 4.116

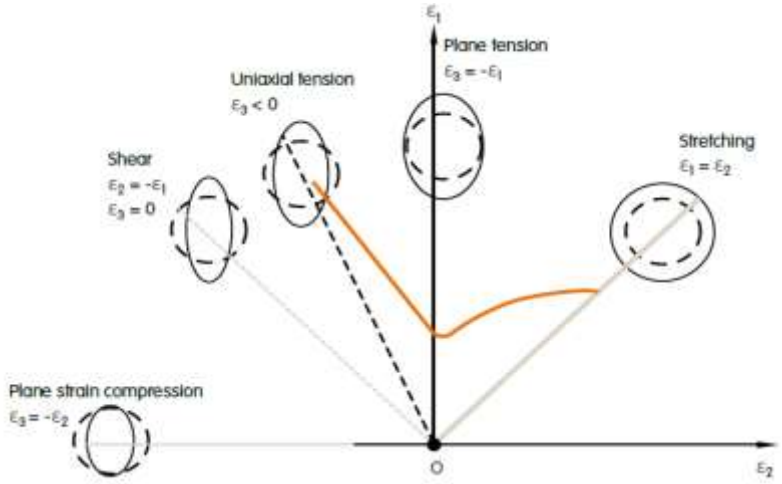

Figure 1: Strain diagram for sheet forming, showing a typical forming limit diagram (FLD).

Most of the nonferrous metals and alloys do not show the sudden bend or kink in their stress strain curve. Instead there is a gradual transition from elastic to plastic state as shown in figure 2. In such cases, the yield strength may be taken at the point of intersection of tangents to elastic and plastic lines [6]. The nominal stress is not the real effective stress, since it represents the instantaneous load divided by the initial specimen section. The nominal strain is not very useful, because it is not additive. The true stress-strain curve describes the homogeneous strain hardening of the material under uniaxial tension (figure 3). The most frequently employed expression is the Ludwik equation:

$$\sigma = \sigma_0 + k\,\varepsilon^n \qquad (2)$$

where σ_0, k and n are constants.

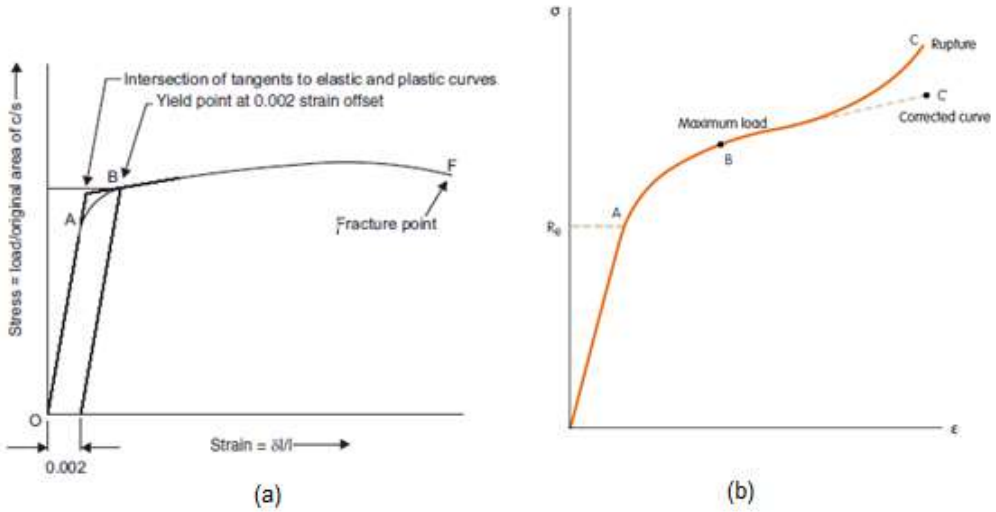

Figure 2: A typical stress-strain curve for aluminum: (a) nominal stress-strain curve and (b) true stress- strain curve.

Single point incremental forming (SPIF) is a rather new sheet metal forming process forming by local stretching of the sheet with a pin tool following a tool path controlled by a CNC machine. In contradiction to traditional deep drawing and stretch forming, where the sheet is formed in a single step operation with a shaped punch and die it is formed incrementally in a multi pass procedure using a single point, rotating tool pin with a spherical tip as shown in figure 3.

ISSN: 2277-9655
Impact Factor: 4.116

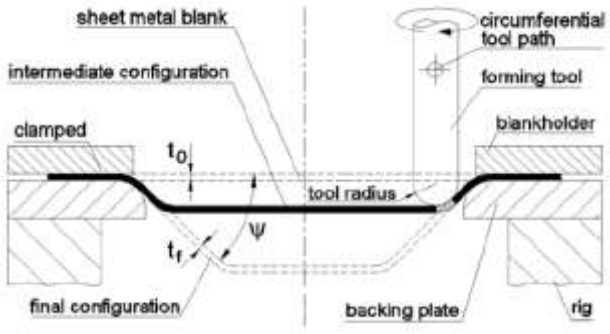

Figure 3: Schematic representation of SPIF.

Main process parameters in SPIF are: tool radius, sheet thickness, drawing angle ψ, and the downwards step size per revolution [7-12]. The sheet metal parts produced by SPIF may have complex shapes but circle grid analysis in conjunction with the observation of the smear-mark interferences between the tool and the surface of the sheet allow the classification of all possible tool paths as combinations of the three basic modes of deformation: (1) flat surfaces under plane strain stretching conditions, (2) rotational symmetric surfaces under plane strain stretching conditions and (3) corners under equal bi-axial stretching conditions, [13].

In this paper, the formability diagram of SPIF forces is presented, based on results derived from the finite element analysis results and validated results obtained from the experimental grid-based deformation for deep drawn pyramidal cups.

MATERIALS AND METHODS

In the present work, ABAQUS (6.14) software code was used for the numerical simulation of SPIF process to fabricate conical cups. The material was AA2004 alloy. The sheet and tool geometry were modeled as deformable and analytical rigid bodies, respectively, using ABAQUS. They were assembled as frictional contact bodies. The sheet material was meshed with S4R shell elements (figure 4a). The fixed boundary conditions were given to all four edges of the sheet as shown in figure 4b. The boundary conditions for tool were x, y, z linear movements and rotation about the axis of tool. True stress-true strain experimental data were loaded in the tabular form as material properties. The tool path geometry was generated using CAM software was imported to the ABAQUS as shown in figure 5. The superplastic deformation analysis was carried out for the equivalent stress, strain and thickness variation. Uniaxial tensile test were conducted to validate FLD diagrams.

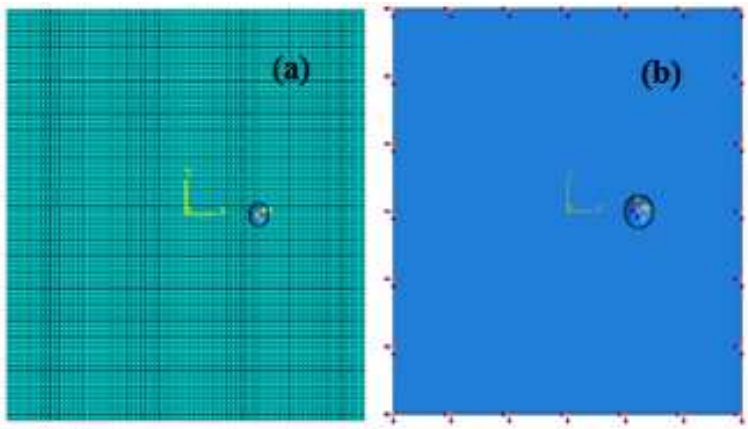

Figure 4: Finite element modeling: (a) mesh generation and (b) boundary conditions.

ISSN: 2277-9655
Impact Factor: 4.116

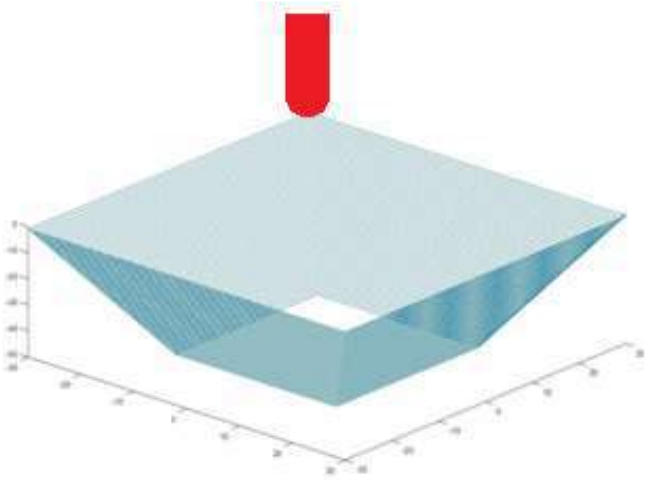

Figure 5: Tool path generation.

RESULTS AND DISCUSSION

For the pyramidal cups, the maximum equivalent stress induced is 269 MPa (figure 6). The maximum equivalent stress was found at the corner edges formed by the side walls of the cups. The major and minor principal stresses, S_{11} (figure 7a) and S_{22} (figure 7b) was compressive in nature except for the strains less than 0.4 which is in the elastic range of AA2004. The shear stress was due to compressive stresses in the blank sheet (figure 7c). The equivalent strain was found to be 2.026 (figure 8) for the pyramidal cup.

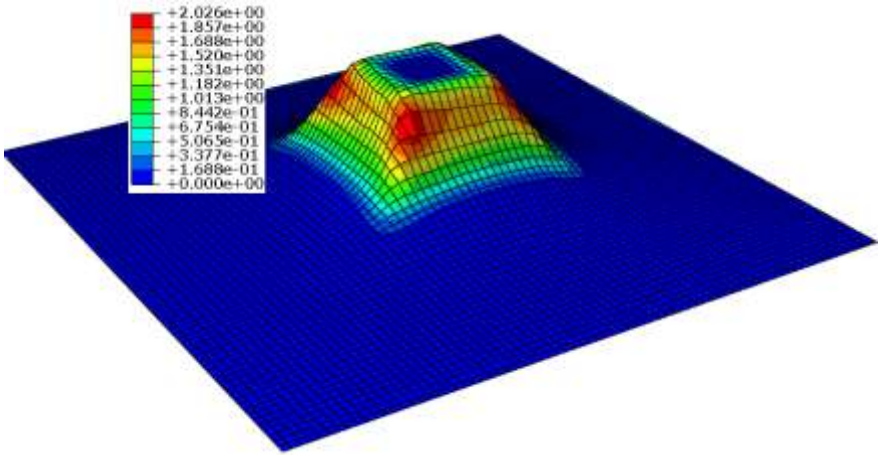

Figure 6: Equivalent stress induced in conical cup.

ISSN: 2277-9655
Impact Factor: 4.116

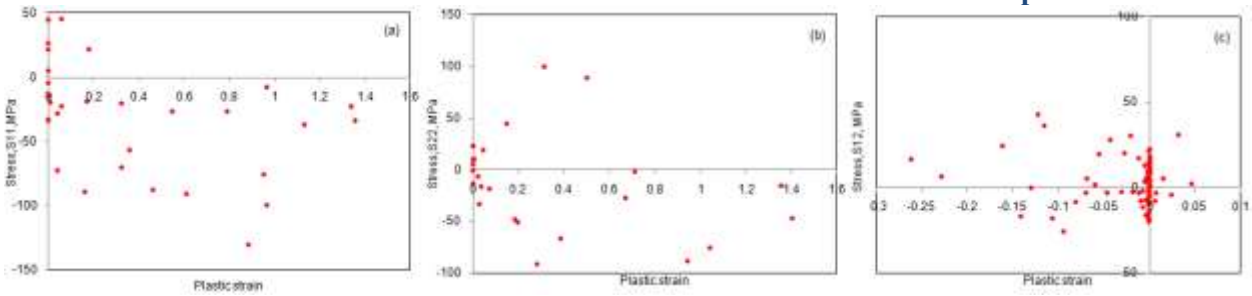

Figure 7: Principal stresses S_{11}, S_{12}, S_{22}

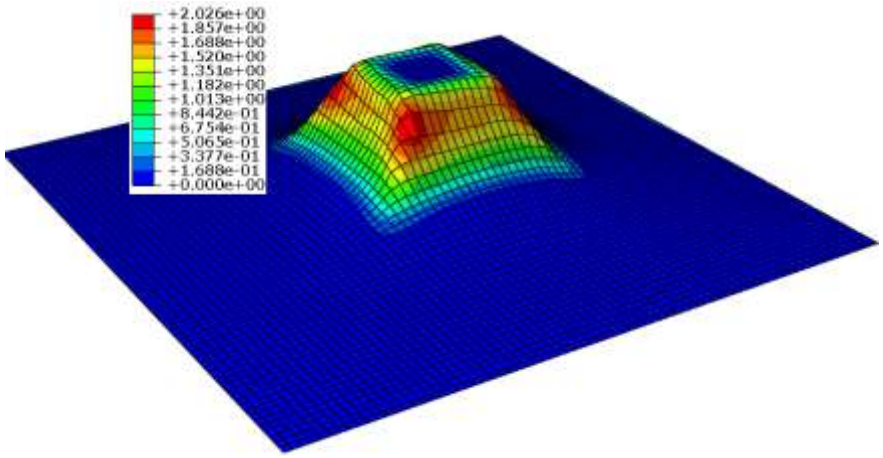

Figure 8: Equivalent strain induced in pyramidal cup.

The finite element grid of 5mm size was created on the backside of the cup material to validate the simulation results. The stress (figure 6) and strain (figure 8) obtained by the finite element method coincides with the pattern (figure 9) on the cups. From the experiments conducted on CNC machine to draw pyramidal cups, the maximum strains was found to be 2.18 without any rupture. Hence, the simulation results were validated. The error in the results was due to difference of element size in the finite element analysis with that used for the experimental grid-based deformation. The element size was 2mm and 5mm, respectively for the finite element analysis and experimentation. Figure 10a presents the major strain along line 6 (defined in figure 10b) for all the 30 incremental forming loops of the truncated pyramid. The major strain increment amplitude increases as the tool moves downwards with a constant depth increment step size of 1 mm. As a consequence, the major strain increases globally along the arrow defined in figure 10b.

ISSN: 2277-9655
Impact Factor: 4.116

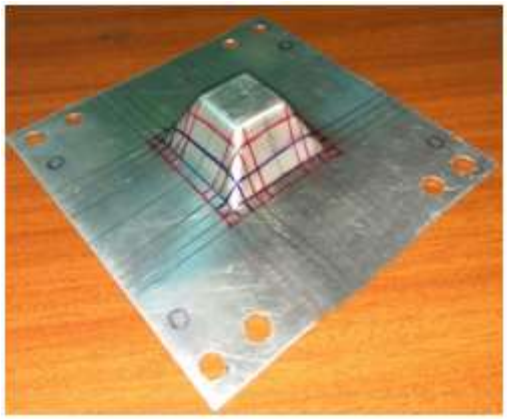

Figure 9: Grid-based deformation on the pyramidal cup drawn on CNC machine.

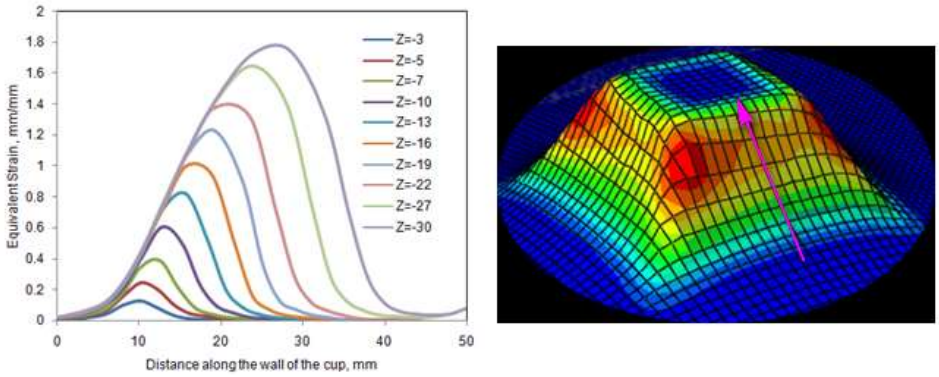

Figure 10: Evolution of the major strain along line 6 for each of the 25 incremental loops.

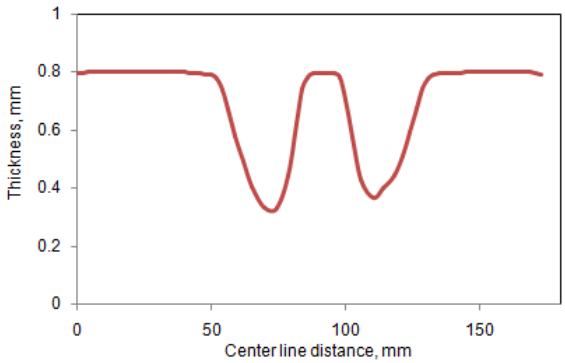

Figure 11: Thickness variation along the walls of conical and pyramidal cups.

The thickness variation along the walls of pyramidal cups is shown in figure 11. The thickness reduction was found to be maximum along the side walls of the cup. It could point out that thinning of SPIF specimen plays a basic role in SPIF process. The thickness reduction in the flange and the bottom of the cups was negligible. Figure 12 represents the formability diagrams of the pyramidal cup deep drawn from AA2004. The formability limit diagram was dominated by the pure shear for the major strain less than 0.5 and by the uni-axial tension for major strain higher than 0.5. Recent studies have shown that the forming limit curve, which describes the formability in a minor-major strain plane, may be expressed as a straight line with a negative slope [14]. In the present case, the deformation mode is very close to plane strain deformation and strain path dependant. For most materials, forming

limit curve intersects the major strain axis at the point equivalent to n-value. As n-value decreases, the limit strain level decreases. For aluminum alloy 2004, the major strain values are approximately 0.12 and 0.14 at plane strain region of the FLD. Frictional effect between the tool and the sheet was considered in the study. Hill's yield criterion and BBC yield criterion stand in good agreement compared to the experimental marginal points, the overall comparison shows a fair agreement between finite element analysis results and data obtained from the experiments. Although the forming behavior of materials can be well expressed through uni-axial tensile tests, the theoretical prediction of FLD may still lie in large deviations from the experimentally determined FLDs.

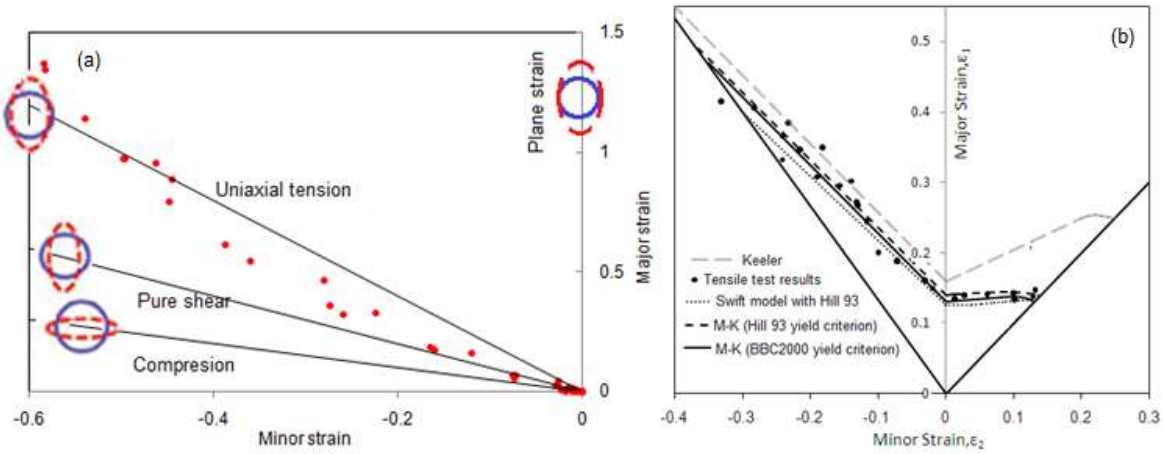

Figure 12: Formability limit diagrams of conical and pyramidal cups: (a) simulation results and (b) tensile test results.

CONCLUSIONS

The forming limit diagram (FLD) of aluminum alloy 2004 was investigated by the single point incremental forming process to fabricate pyramidal cups. The influences of strain path on forming limits were studied by considering proportional strain path. The present investigation confirms that the FLD is sensitive to strain path of aluminum alloy 2004. During the calculation of stress for FLD from measured strain, both the hardening law and yield criterion are essential influence factors. For aluminum alloy 2004 alloy, the best agreement between experimental and theoretical approaches was achieved when the M-K with Hill'93 yield criteria was used. As a result, the overall comparison shows a well agreement between finite element analysis results and data obtained from the experiments.

ACKNOWLEDGEMENTS

The author acknowledges with thanks University Grants Commission (UGC) – New Delhi for financial support of this R&D project.

REFERENCES

1. A. C. Reddy, "Evaluation of local thinning during cup drawing of gas cylinder steel using isotropic criteria," International Journal of Engineering and Materials Sciences, Vol.5, No.2, pp.71-76, 2012.
2. A. C. Reddy, "High temperature and high strain rate superplastic deep drawing process for AA2618 alloy cylindrical cups," International Journal of Scientific Engineering and Applied Science, Vol.2, No.2, pp.35-41, 2016
3. A. C. Reddy, "Practicability of High Temperature and High Strain Rate Superplastic Deep Drawing Process for AA3003 Alloy Cylindrical Cups," International Journal of Engineering Inventions, Vol.5, No.3, pp.16-23, 2016
4. A. C. Reddy, "High temperature and high strain rate superplastic deep drawing process for AA5049 alloy cylindrical cups," International Journal of Engineering Sciences & Research Technology, Vol.5, No.2, pp.261-268, 2016

5. A. C. Reddy, "Suitability of High Temperature and High Strain Rate Superplastic Deep Drawing Process for AA5052 Alloy," International Journal of Engineering and Advanced Research Technology, Vol.2, No.3, pp.11-14, 2016.
6. U. Saeed and J. G. Lenard, "A Comparison of Cold Rolling Theories Based on the Equilibrium Approach," Journal of Engineering Materials And Technology, Vol. 102, pp. 223–228, 1980.
7. T. Santhosh Kumar and A. C. Reddy, "Finite Element Analysis of Formability of Pyramidal Cups Fabricated from AA1100-H18 Alloy, International Journal of Science and Research," Vol.5, No.6, pp.1172-1177, 2016
8. A. Raviteja and A. C. Reddy, "Finite Element Analysis of Single Point Incremental Deep Drawing Process for Truncated Pyramidal Cups from AA 1070 Alloy," International Journal of Innovative Science, Engineering & Technology, Vol.3, No.6, pp.263-268, 2016
9. V. Srija and, A. C. Reddy, "Numerical simulation of truncated pyramidal cups of AA1050-h18 alloy fabricated by single point incremental forming," International Journal of Engineering Sciences & Research Technology, Vol.5, No.6, pp.741-749, 2016
10. T. Santhosh Kumar and A. C. Reddy, "Single Point Incremental Forming and Significance of its Process Parameters on Formability of Conical Cups Fabricated From AA1100-H18 Alloy," International Journal of Engineering Inventions, Vol.5, No.6, pp.10-18, 2016
11. A. Raviteja and A. C. Reddy, "Implication of process parameters of single point incremental forming for conical frustum cups from AA1070 using FEA," International Journal of Research in Engineering and Technology, Vol.5, No.6, pp.124-129, 2016
12. T. Santhosh Kumar, V. Srija, A. Ravi Teja and A. C. Reddy, "Influence of Process Parameters of Single Point incremental Deep Drawing Process for Truncated Pyramidal Cups from 304 Stainless Steel using FEA," International Journal of Scientific & Engineering Research, Vol.7, No.6, pp.100-105, 2016
13. C. R. Alavala, "FEM analysis of single point incremental forming process and validation with grid-based experimental deformation analysis," International Journal of Mechanical Engineering, Vol.5, No.5, pp.1-6, 2016.
14. L. Filice, L. Fantini and F. Micari, "Analysis of Material Formability in Incremental Forming," Annals of the CIRP, vol. 51, No.1, pp.199-202, 2002.